Hindawi
Shock and Vibration
Volume 2020, Article ID 9270318, 12 pages
https://doi.org/10.1155/2020/9270318

Research Article

Vibration Characteristic Analysis of Pressure Fluctuating Attenuator with Circular Elastic Sheets for Linear-Driving Pump

Songlin Nie,[1] Lianwei Li,[1] Hui Ji,[1] Fanglong Yin,[1] and Zhaoyi Dai[2]

[1]*Beijing Key Laboratory of Advanced Manufacturing Technology, Beijing University of Technology, Beijing 100124, China*
[2]*Rice University, Department of Civil and Environmental Engineering, 6100 Main Street, Houston, TX, USA*

Correspondence should be addressed to Hui Ji; jihui@bjut.edu.cn

Received 22 October 2019; Revised 26 June 2020; Accepted 8 July 2020; Published 24 July 2020

Academic Editor: Miguel Neves

Aiming at the problem of pipeline vibration caused by fluids in linear-driving pump pipeline system, this paper proposed a vibration reduction method based on a pressure-fluctuating attenuator with circular elastic sheets. Firstly, a new type of pressure-fluctuating attenuator was proposed, and its working principle and frequency characteristics were analyzed. Secondly, the mathematical model of the developed attenuator was established in combination with the dynamic characteristic equations of the pipeline. Besides, the effect of relevant parameters on attenuation performance was investigated through simulation. The size and material of the circular elastic sheet were screened according to the pressure fluctuating frequency of the linear-driving pump under the rated conditions. The prototype of the pressure-fluctuating attenuator was fabricated, and the performance of the prototype in the pipeline was tested. The experimental results show that the pressure-fluctuating attenuator with circular elastic sheets has a good suppression effect on the pulsating pressure of the linear-driving pump under the rated conditions.

1. Introduction

Water hydraulic piston pump is widely used in lots of industrial fields because it has many advantages such as cleanliness, safety, high volume efficiency, and high power density. As a new type of bilge drainage pump, a water hydraulic piston pump driven by linear motors (referred to as linear-driving pump) breathes and removes water through the reciprocating motion of pistons. In comparison with the conventional pump, the linear-driving pump does not need any transformation devices. Therefore, its vibration is slight, while its efficiency is high. However, the inertia shock is inevitable when the motion direction of the high-speed linear-driving pump changes. Besides, shock vibration is inevitable too because of the high-frequency opening and closing of the flow valves [1, 2]. These vibrations will be transmitted to the body of the device through pipeline [3, 4], which will not only decrease the concealment performance of the device but also have influence on the health and living environment of the staff. Therefore, the vibration characteristics and research of vibration reduction on the pipeline of the linear-driving pump are significant to enhance the reliability of the pipeline.

In order to suppress the vibration and noise propagation in the pipeline, various pulsation attenuators have been developed [5–9], such as collateral resonator, Helmholtz muffler, multihole concentric muffler, multicavity resonator, the pulsation filtering structure derived from expansion tube, expansion muffler, and single expansion cavity muffler. For example, Bi et al. [10] proposed a perforated silencing structure, when the sound wave entered the small holes, and the air vibration in the cavity was excited to achieve the attenuation of noise. Zhang et al. [11] proposed a concentric porous pressure pulsation attenuator, which achieved a wider attenuation band by applying a perforated tube structure to hydraulic pressure pulsation attenuation.

Generally, the pressure fluctuating attenuator was employed to reduce the pulsation pressure amplitude. Josef [12] designed a pressure pulsation attenuator for the hydraulic system, whose working principle was to connect a cavity in the pipeline of the hydraulic system, and a piston type vibration mass was placed in the cavity; its action

mechanism was similar to the damped vibration absorber. He et al. [13] and Sang [14] proposed a circular sheet resonant pulsation attenuator, which used a sheet structure to absorb small pulsation vibration and the pulsating energy in the system. The cavity structure of the H-type muffler was retained, and the combination of structure and cavity pulsation attenuation was realized. Sripriya et al. [15] carried out a study on structural acoustic muffler, which was verified experimentally to attenuate the pulsation of a wider frequency band. Ren and Cao [16] researched and analyzed the working mechanism and performance of the porous resonant pressure-fluctuating attenuator. Zhang [17] established H-type and multihole concentric pulsation attenuator models based on the frequency method and finite element simulation, respectively, and analyzed the influence of structural parameters on the performance of the pulsation attenuator. He et al. [18] designed a pulsation attenuator based on the principle of cochlear basement membrane simulation, analyzed the influence of structural parameters on the performance of the attenuator, and verified its broad-spectrum filtering characteristics through experiments.

In this study, the vibration control strategy induced by the pipeline flow of the linear-driving pump is studied. Firstly, the working principle of the pressure-fluctuating attenuator with circular elastic sheets is introduced, and by deducing the natural frequency formula of the circular elastic sheets with fixed boundary in the pressure-fluctuating attenuator, the variation of the natural frequency is analyzed from the thickness and radius of the circular elastic sheet, respectively. Secondly, based on the transfer equation of the pressure-fluctuating attenuator and the pipeline system, the mathematical model of the entire vibration damping system is established, and the vibration damping performance of the pressure fluctuating attenuator is analyzed using the insertion loss as the evaluation standard. By analyzing the vibration frequency characteristics of the linear motor pump under different load conditions, the pressure-fluctuating attenuator is developed. Finally, the effectiveness of the attenuator is verified by experiments, and a control method is proposed for the low-frequency pulse amplitude generated under low-pressure load conditions.

2. Work Principle and Natural Frequency Characteristics

2.1. Working Principle. According to the frequency characteristics of the pipeline system of the linear-driving pump, a new type of the pressure-fluctuating attenuator with circular elastic sheets is proposed (as shown in Figure 1).

The pressure-fluctuating attenuator is mainly composed of shell, circular elastic sheet, a static pressure balance hole, and gland with O-ring. The shell is made from stainless steel and encloses a main cavity. A circular concave is formed around the shell, and the circular elastic sheet is placed on the circular concave table and pressed by the gland. A static pressure balance chamber is enclosed between the circular elastic sheet and the gland. The main cavity and the static pressure balance chamber are connected through a static pressure balance hole so that the water flow is performed on both sides. When the fluctuating pressure in the main cavity acts on the circular elastic sheet, the sheet will interact with the surrounding fluid and cause vibration of the fluid. When the frequency of fluctuating pressure in the chamber is identical or close to the natural frequency of the circular elastic sheet, the sheet will resonate and consume the fluctuating pressure to achieve the effect of vibration attenuation.

2.2. Natural Frequency Characteristics. According to the principle of the pressure-fluctuating attenuator, the circular elastic sheet is the core element of the attenuator and its natural frequency has an important influence on the attenuation effect of fluctuating pressure. The normal frequency formula for the vibration of the circular elastic sheet with a fixed boundary can be derived [19, 20], which can accurately describe the vibration characteristics of the circular elastic sheet:

$$f_n = \frac{u_n^2 h}{4\pi a^2}\sqrt{\frac{E}{3\rho_p(1-\mu^2)}}, \tag{1}$$

where u_n is the root of the zero-order cylindrical Bessel function, E is Young's modulus, h is the thickness of sheet, a is the radius of sheet, ρ_p is the quality density of sheet, and μ is Poisson's ratio. On the basis of the cylindrical Bessel function and the virtual variables' Bessel function value distribution table, the value of the root of the zero-order Bessel function can be obtained. Among them, $u_1 = 3.2$, $u_2 = 6.3$, and $u_3 = 9.44$; when n is greater than 3, $u_n = n\pi$. The fundamental frequency of free vibration of the circular elastic sheet can be expressed as follows:

$$f_1 = \frac{(3.2)^2 h}{4\pi a^2}\sqrt{\frac{E}{3\rho_p(1-\mu^2)}} = 0.467\frac{h}{a^2}\sqrt{\frac{E}{\rho_p(1-\mu^2)}}. \tag{2}$$

Differing from the free vibration, when the circular elastic sheet is surrounded by fluid, the vibration of the sheet will cause vibration of fluid on both sides, which will decrease the vibration of the sheet and the natural frequency of each order. The fluctuating pressure causes the vibration and deformation of the sheet, which will affect the distribution of the fluid. Therefore, when studying the vibration of the circular elastic sheet in fluctuating fluid, it is necessary to comprehensively consider the interaction of the sheet and the fluid.

When the fluctuating pressure of the system induces the forced vibration of the circular elastic sheet, the dimensionless vibration displacement corresponding to the normal frequency of each step can be expressed as follows [19]:

$$w_{\mathrm{nm}}(r) = \left(P_{\mathrm{nm}}J_n\left(\frac{u_{\mathrm{nm}}r}{a}\right) + Q_{\mathrm{nm}}I_n\left(\frac{u_{\mathrm{nm}}r}{a}\right)\right)e^{j\omega_{\mathrm{nm}}t}. \tag{3}$$

When circular elastic sheet satisfies the normal model state, equation (3) can be rewritten as follows [19]:

$$w_{\mathrm{nm}}(r) = G_{\mathrm{nm}}\left[J_n\left(\frac{u_{\mathrm{nm}}r}{a}\right) - \frac{J_n(u_{\mathrm{nm}})}{I_n(u_{\mathrm{nm}})}I_n\left(\frac{u_{\mathrm{nm}}r}{a}\right)\right]e^{j\omega_{\mathrm{nm}}t}, \tag{4}$$

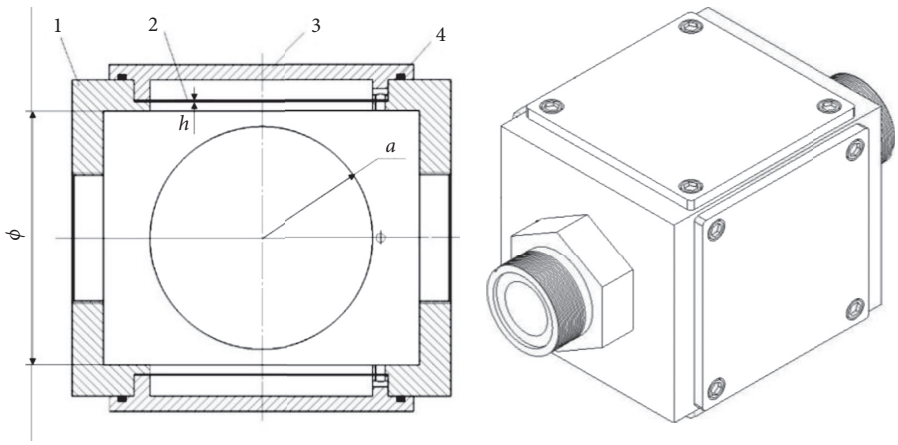

Figure 1: Structure diagram of pressure-fluctuating attenuator. (a) Sectional view. (b) Three-dimensional view.

where J_n is n-order Bessel function, I_n is virtual variables Bessel function, G_{nm} is the maximum vibration displacement amplitude of the circular elastic sheet at any point in nm-order modal vibration, r is the radius of a certain point of sheet, u_{nm} is the root of the cylindrical Bessel function satisfying the normal equation, and P_{nm} and Q_{nm} are the undetermined parameters. Here, G_{nm} is represented by the average displacement $\overline{w}_n$ [19]:

$$G_{\mathrm{nm}} = \frac{\overline{w}_n u_n}{2}\left[J_1(u_n) - \frac{J_0(u_n)}{I_0(u_n)} I_1(u_n)\right]^{-1}. \tag{5}$$

Equation (4) expressed in power series can be simplified as follows [19, 21]:

$$w_{\mathrm{nm}}(r) = G_{\mathrm{nm}}\left(1 + \alpha\frac{r^2}{a^2} + \beta\frac{r^4}{a^2}\right)e^{j\omega t}, \tag{6}$$

where $\alpha = -(u_n^4/4)((I_n(u_{\mathrm{nm}}) - J_n(u_{\mathrm{nm}}))/(I_n(u_{\mathrm{nm}}) + J_n(u_{\mathrm{nm}})))$, $\beta = (u_n^4/64)((I_n(u_{\mathrm{nm}}) + 16J_n(u_{\mathrm{nm}}))/(I_n(u_{\mathrm{nm}}) + J_n(u_{\mathrm{nm}})))$.

Under the action of the fluctuating pressure, the potential energy H_P, kinetic energy T_P of the circular elastic sheet, and kinetic energy T_w of the fluid on both sides of the circular elastic sheet are shown by equations (7)–(9), respectively [19]:

$$H_P = \frac{D}{2\pi a^2} B_{\mathrm{nm}} \overline{w_{\mathrm{nm}}^2}, \tag{7}$$

$$T_P = \frac{\pi\rho_p h a^2}{2}\left[(\overline{w_{\mathrm{nm}}})'\right]^2 A_{\mathrm{nm}}, \tag{8}$$

$$T_w = \pi\rho_p h a^2\left[(\overline{w_{\mathrm{nm}}})'\right]^2 \frac{\rho_w a}{\rho_p h}\frac{8}{3\pi} C_{\mathrm{nm}}, \tag{9}$$

where B_{nm} is the potential energy factor of circular elastic sheet with a fixed boundary, A_{nm} is the kinetic energy factor of circular elastic sheet with a fixed boundary, C_{nm} is the kinetic energy factor of the sheet, ρ_w is the density of the fluid, and D is the bending stiffness of the sheet.

According to the principle of virtual work, in the process of interaction between the circular elastic sheet and the fluid, the kinetic energy excited by the fluctuating fluid is equal to the sum of the kinetic energy and potential energy of the sheet [19]:

$$\frac{\partial H_P}{\partial \overline{w}}\delta\overline{w} + \frac{\partial T_P}{\partial \overline{w}}\delta\overline{w} + \frac{\partial T_w}{\partial \overline{w}}\delta\overline{w} = pe^{j\omega t}. \tag{10}$$

Substituting equations (7)–(9) into equation (10), we have

$$\begin{aligned}&\frac{D}{\pi a^2} B_{\mathrm{nm}} \overline{w_{\mathrm{nm}} w_{\mathrm{nm}}}' + \rho_p h\pi a^2 A_{\mathrm{nm}} \overline{w_{\mathrm{nm}}}' \overline{w_{\mathrm{nm}}}'' \\ &+ \rho_p h a^2 \frac{8\rho_w a}{3\rho_p h} C_{\mathrm{nm}} \overline{w_{\mathrm{nm}}}' \overline{w_{\mathrm{nm}}}'' = Fe^{j\omega t},\end{aligned} \tag{11}$$

where $p = F/\pi a^2$ and $v = \overline{w_{\mathrm{nm}}}' = \int \overline{w_{\mathrm{nm}}}'' \mathrm{d}t$.

The Laplace transform of equation (11) can be obtained as follows [19]:

$$\begin{aligned}&-\frac{jD}{\omega(\pi a^2)^2}\overline{w_{\mathrm{nm}}}' B_{\mathrm{nm}} + j\omega\rho_p h \overline{w_{\mathrm{nm}}}' A_{\mathrm{nm}} \\ &+ j\omega\rho_p h \frac{\rho_w a}{\rho_p h}\frac{8}{3\pi}\overline{w_{\mathrm{nm}}}' C_{\mathrm{nm}} = pe^{j\omega t},\end{aligned} \tag{12}$$

When the impedance of the circular elastic sheet with a fixed boundary takes a minimum value, the normal frequency of the vibration is shown as follows [19]:

$$f_P = \frac{u_{\mathrm{nm}}^2 h}{4\pi a^2}\sqrt{\frac{E}{3\rho_p(1+\Gamma)(1-\mu^2)}}, \tag{13}$$

where fluid-loaded coefficient of the circular elastic sheet is $\Gamma = 8\chi a\rho_w/(3\pi h\rho_P)$ and fluid-loaded factor coefficient is $\chi = (C_{\mathrm{nm}}/A_{\mathrm{nm}})$.

When the circular elastic sheet with fixed boundary vibrates at low frequency, the value of the fluid-loaded coefficient χ corresponding to each modal is shown in Table 1:

Table 1: Fluid-loaded coefficients of the circular elastic sheet with fixed boundary.

χ	$n=0$	$n=1$	$n=2$	$n=3$
$m=1$	0.5502	0.3216	0.2356	0.1861
$m=2$	0.2392	0.1803	0.1461	0.1249
$m=3$	0.1496	0.1237	0.1060	0.0931
$m=4$	0.1072	0.0931	0.0836	0.0754

The equations (3) and (13) were processed by MATLAB to obtain the influence of the thickness and radius of the circular elastic sheet with fixed boundary on the normal frequency under the free vibration and fluid-loaded conditions, as shown in Figure 2. Here, Young's modulus of the sheet is 1.95×10^{11} Pa, while Poisson's ratio is 0.3 and the density is 7930 Kg/m^3.

As shown in Figure 2, under the conditions of free vibration and fluid-loaded vibration, the normal frequency of the circular elastic sheet with a fixed boundary increases with the increase of the thickness of the sheet and increases with the decrease of the radius of the sheet. However, due to the influence of the fluid-loaded factor, the normal frequency of the sheet with the same structural parameters under the fluid-loaded condition is much smaller than the normal frequency under the condition of free vibration.

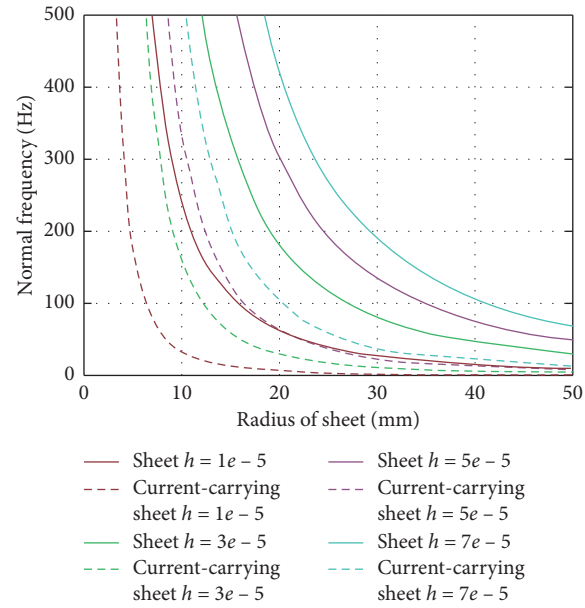

Figure 2: Effect of radius and thickness on normal frequency of sheet under different conditions.

3. Model Establishment and Simulation Analysis

3.1. Model Establishment and Performance Simulation

3.1.1. Mathematical Model. The pressure-fluctuating attenuator studied in this paper belongs to the resistance attenuator [22], which does not contain damping material. Therefore, the pressure-fluctuating attenuator is composed of straight pipe, starting cavity, and throttling orifice. The mathematical model of the pressure-fluctuating attenuator was established based on the dynamic mathematical model of each unit. Equivalent model of pressure-fluctuating attenuator with sheets is shown in Figure 3.

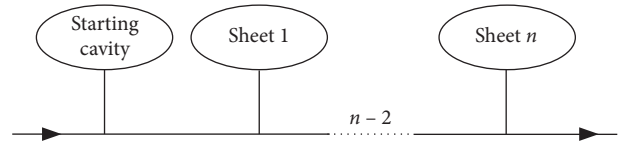

Figure 3: Equivalent model of the pressure-fluctuating attenuator with sheets.

As shown in Figure 3, the mathematical model of the pressure-fluctuating attenuator with sheets [23] can be expressed as follows:

$$\begin{pmatrix} P_i(s) \\ Q_i(s) \end{pmatrix} = \begin{pmatrix} 1 & 0 \\ \dfrac{Vs}{K_e} & 1 \end{pmatrix} \times \begin{pmatrix} 1 & 0 \\ \sum_{i=1}^{n} Y_i(s) & 1 \end{pmatrix} \begin{pmatrix} P_o(s) \\ Q_o(s) \end{pmatrix}, \tag{14}$$

where V is the volume of main cavity, $Y_i(s)$ is the inlet admittance at the shunt caused by vibration of the resonant sheet, P_i is the inlet pressure, P_o is the outlet pressure, K_e is the volume elastic modulus of fluid medium, Q_i is the inlet flow, and Q_o is the outlet flow.

Among them, $Y_i(s)$ is determined by the vibration characteristics of the sheet. As shown in Figure 4, on the fluid-solid interaction surface, the fluctuating pressure of the fluid causes deformation and vibration of the sheet.

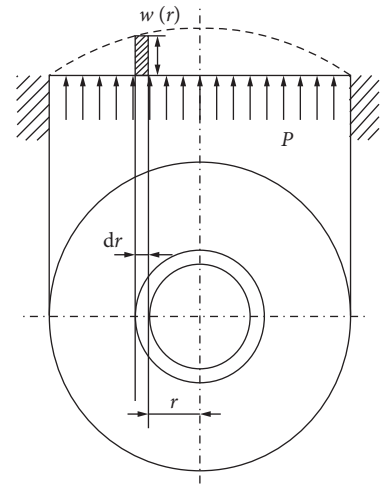

Figure 4: Diagram of deformation of the circular elastic sheet in fluid.

Meanwhile, the deformation and vibration of the sheet will cause pulsation of the flow and pressure of the fluid.

Considering the deformation of the sheet in the pressure-fluctuating attenuator is a small disturbance deformation, the influence of the steady flow velocity of the parallel flow through the sheet on the vibration can be

neglected, and the vibration displacement of the sheet under the fluctuating pressure can be derived as follows [24, 25]:

$$w(r) = \left(\frac{P}{64D} + \frac{\rho v_0^2}{64D}\right)\left(a^4 - 2a^2r^2 + r^4\right), \tag{15}$$

$$D = \left(\frac{\mathrm{Eh}^3}{12(1-\mu^2)}\right), \tag{16}$$

where v_0 is the velocity of fluid flows through the sheet in parallel, P is the pressure of the fluid, a is the radius of the sheet, h is thickness of the sheet, D is bending stiffness of the sheet, E is elastic modulus of the sheet, and μ is Poisson's ratio of the sheet.

In the actual system, ρv_0^2 is smaller than P, equation (15) can be simplified as follows:

$$w(r) = \frac{\mathrm{Pa}^4}{64D}\left(1 - \frac{r^2}{a^2}\right)^2. \tag{17}$$

The change in volume of the liquid caused by the vibration of the sheet is

$$V = \int_0^a 2\pi r w(r)\mathrm{d}r. \tag{18}$$

Substituting equation (17) into equation (18), we can be obtain

$$\mathrm{d}V = \frac{a^6\pi}{192D}\mathrm{d}P. \tag{19}$$

Substitute $\mathrm{d}V = Q\mathrm{d}t$ into equation (19):

$$Q = \frac{a^6\pi}{192D}\frac{\mathrm{d}P}{\mathrm{d}t}. \tag{20}$$

The Laplace transform of equation (20) can be expressed as follows:

$$Q(s) = \frac{a^6\pi}{192D}sP(s). \tag{21}$$

The admittance at the shunt can be derived from equation (21):

$$Y(s) = \frac{Q(s)}{P(s)} = \frac{a^6\pi}{192D}s. \tag{22}$$

The transfer matrix of the fluctuating-pressure attenuator with sheets is

$$\begin{aligned} \mathrm{T} &= \begin{pmatrix} 1 & 0 \\ \dfrac{Vs}{K_e} & 1 \end{pmatrix} \times \begin{pmatrix} 1 & 0 \\ \sum_{i=1}^{n} Y_i(s) & 1 \end{pmatrix} \\ &= \begin{pmatrix} 1 & 0 \\ \dfrac{Vs}{K_e} & 1 \end{pmatrix} \times \begin{pmatrix} 1 & 0 \\ \sum_{i=1}^{n} \dfrac{a_i^6\pi s}{192D_i} & 1 \end{pmatrix}. \end{aligned} \tag{23}$$

3.1.2. Performance Simulation of the Pressure-Fluctuating Attenuator. The pipeline is equipped with the linear-driving pump and the pressure-fluctuating attenuator is shown in Figure 5.

According to Figure 5, the transfer equation of the pipeline system is shown in equations (24) and (25):

$$\begin{aligned} \begin{pmatrix} P_1 \\ Q_1 \end{pmatrix} &= \begin{pmatrix} A_{11} & A_{12} \\ A_{21} & A_{22} \end{pmatrix} \times \begin{pmatrix} T_{11} & T_{12} \\ T_{21} & T_{22} \end{pmatrix} \times \begin{pmatrix} B_{11} & B_{12} \\ B_{21} & B_{22} \end{pmatrix} \times \begin{pmatrix} P_2 \\ Q_2 \end{pmatrix} \\ &= \begin{pmatrix} S_{11} & S_{12} \\ S_{21} & S_{22} \end{pmatrix} \times \begin{pmatrix} P_2 \\ Q_2 \end{pmatrix}, \end{aligned} \tag{24}$$

$$\begin{pmatrix} P_2 \\ Q_2 \end{pmatrix} = \begin{pmatrix} D_{11} & D_{12} \\ D_{21} & D_{22} \end{pmatrix} \times \begin{pmatrix} P_3 \\ Q_3 \end{pmatrix}, \tag{25}$$

where $L1, L2$, and $L4$ are the lengths of the stainless-steel pipeline system, P and Q are the fluctuating pressure and flow of each measuring point of the linear-driving pump, and the matrices A, B, D, T, and S are the functions of the pipeline system structure parameters.

When the pressure-fluctuating attenuator in Figure 5 was replaced by a stainless-steel straight pipeline of length L_3, the transfer equation of the linear-driving pump pipeline system with the pressure fluctuating attenuator can be expressed as follows:

$$\begin{aligned} \begin{pmatrix} P_1' \\ Q_1' \end{pmatrix} &= \begin{pmatrix} A_{11} & A_{12} \\ A_{21} & A_{22} \end{pmatrix} \times \begin{pmatrix} C_{11} & C_{12} \\ C_{21} & C_{22} \end{pmatrix} \times \begin{pmatrix} B_{11} & B_{12} \\ B_{21} & B_{22} \end{pmatrix} \times \begin{pmatrix} P_2' \\ Q_2' \end{pmatrix} \\ &= \begin{pmatrix} S_{11}' & S_{12}' \\ S_{21}' & S_{22}' \end{pmatrix} \times \begin{pmatrix} P_2' \\ Q_2' \end{pmatrix}, \end{aligned} \tag{26}$$

where P' and Q' are the fluctuating pressure and flow at the measuring point, respectively.

To study the performance of the attenuator, the insertion loss was chosen as the measuring standard [26]. Insertion loss is the ratio of the fluctuating pressure at the load end of the hydraulic system when the pulsation attenuator was not installed to the fluctuating pressure at the load end and when the pressure-fluctuating attenuator was installed. It can be expressed as follows:

$$IL = 20\lg\left|\frac{\Delta P_0}{\Delta P_m}\right|, \tag{27}$$

where IL is the insertion loss, ΔP_0 is the pulsating pressure at the load end of the pipeline without the pressure fluctuating attenuator, and ΔP_m is the fluctuating pressure at the load end of the pipeline with the pressure-fluctuating attenuator.

It can be deduced from equation (25):

$$P_2 = D_{11}P_3 + D_{12}Q_3, \tag{28}$$

$$Q_2 = D_{21}P_3 + D_{22}Q_3, \tag{29}$$

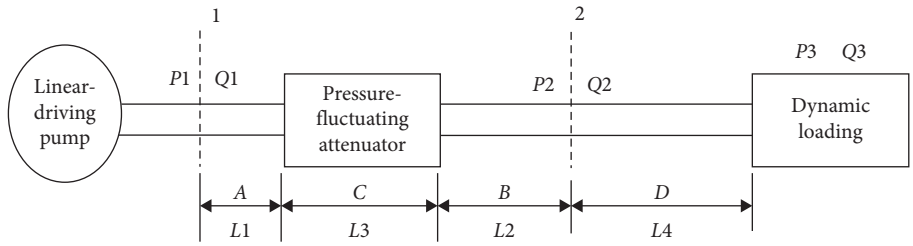

Figure 5: Diagram of the pipeline with pressure-fluctuating attenuator.

$$\frac{Q_2}{P_2} = \frac{D_{21}P_3 + D_{22}Q_3}{D_{11}P_3 + D_{12}Q_3} = \frac{D_{21}Z_v(s) + D_{22}}{D_{11}Z_v(s) + D_{12}} = \frac{2\Delta P_T D_{21} + Q_T D_{22}}{2\Delta P_T D_{11} + Q_T D_{12}}, \tag{30}$$

where ΔP_T is the pressure loss of throttle valve and Q_T is the flow thought the throttle valve.

It can be derived from equations (24) and (30) that

$$\frac{Q_1(s)}{P_2(s)} = S_{21} + S_{22}\frac{Q_2(s)}{P_2(s)} = S_{21} + S_{22}\frac{2\Delta P_T D_{21} + Q_T D_{22}}{2\Delta P_T D_{11} + Q_T D_{12}}. \tag{31}$$

Similarly, it can be derived from equations (26) and (30) that

$$\frac{Q_1'(s)}{P_2'(s)} = S_{21}' + S_{22}'\frac{Q_2'(s)}{P_2'(s)} = S_{21}' + S_{22}'\frac{2\Delta P_T D_{21} + Q_T D_{22}}{2\Delta P_T D_{11} + Q_T D_{12}}. \tag{32}$$

Keeping the linear-driving pump condition unchanged, it can be considered that the fluctuating flow at the measuring point 1 is same. Therefore, the insertion loss of the linear-driving pump with pressure-fluctuating attenuator can be expressed as follows:

$$\mathrm{IL} = 20\lg\left|\frac{P_2'(s)}{P_2(s)}\right| = 20\lg\left|\frac{S_{21} + S_{22}\left(\left(2\Delta P_T D_{21} + Q_T D_{22}\right)/\left(2\Delta P_T D_{11} + Q_T D_{12}\right)\right)}{S_{21}' + S_{22}'\left(\left(2\Delta P_T D_{21} + Q_T D_{22}\right)/\left(2\Delta P_T D_{11} + Q_T D_{12}\right)\right)}\right|. \tag{33}$$

According to equation (33), the influence of parameters such as the radius of the sheet and the volume of the main cavity on the attenuator performance was analyzed. The relevant structural parameters are shown in Table 2.

(1) Effect of the sheet radius on attenuator performance

The radius of the sheets was taken as 36 mm, 40 mm, and 44 mm, respectively, keeping the other simulation parameters constant. The curve of the insertion loss of each size sheets as the function of fluctuating pressure frequency is shown in Figure 6. It can be seen from Figure 6, as the radius of the sheet increases, the peak of the insertion loss also increases slightly, and because the natural frequency of the sheet decreases as the diameter increases, the frequency of resonance with the fluctuating pressure also decreases and the frequency of the fluctuating pressure corresponding to the peak of the insertion loss gradually decreases. The frequency of the peak value is corresponding to the natural frequency of the circular elastic sheet calculated by equation (13).

(2) Effect of the main cavity on attenuator performance

The volume of the main cavity was taken as 0.7 L, 1.4 L, and 2.1 L, respectively, keeping the other simulation parameters constant. The curve of the insertion loss of the different volume as the function of fluctuating pressure frequency is shown in Figure 7. It can be seen from Figure 7 that, as the volume of the main cavity increases, the insertion loss value increases slightly at the same frequency, and because the main cavity has weak effect on the natural frequency of the sheets, the volume of the main cavity has less influence on the insertion loss.

3.2. Prototype Design. The circular elastic sheet acts as the core component of the attenuator; its structural parameters determine the attenuator performance. According to the working principle of the attenuator, when the natural frequency of the circular elastic sheet is the same as the fluctuating pressure frequency, the thin plate will resonate and consume the maximum fluctuating pressure. The radius and thickness of the circular elastic sheet should be selected according to the frequency domain characteristics of the fluctuating pressure under the rated condition of the linear-driving pump.

The pressure transmitter was used to collect the pressure signal at the outlet of the linear-driving pump under rated conditions, and the average component was subtracted to obtain the time domain distribution of the fluctuating component pressure. Using MATLAB to perform Fast Fourier Transform (FFT) on the acquired time domain signal, filtering out the interference of the high-frequency electromagnetic signal of the motor, the frequency domain characteristics of the fluctuating pressure can be obtained, as shown in Figure 8.

Table 2: Simulation parameters.

	Category	Value	Unit
Sheet	Density	7930	kg/m^3
	Young's modulus	1.95e11	Pa
	Poisson's ratio	0.3	—
	Thickness	0.03	mm
	Radius	36	mm
Water	Density	998.2	kg/m^3
	Kinematic viscosity (20°C)	1.006$e-6$	m^2/s
	Bulk modulus of elasticity	2.18e9	Pa
Pipeline	Radius	0.025	m
	Length of section A	0.18	
	Length of section B	0.18	
	Length of section C	0.15	
	Length of section D	1.2	
Main cavity	Volume	0.7	L

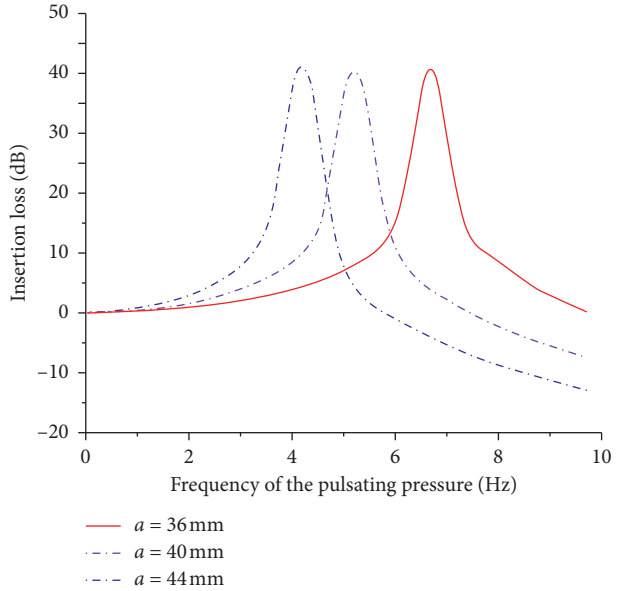

Figure 6: Effect of radius of the sheet on insertion loss.

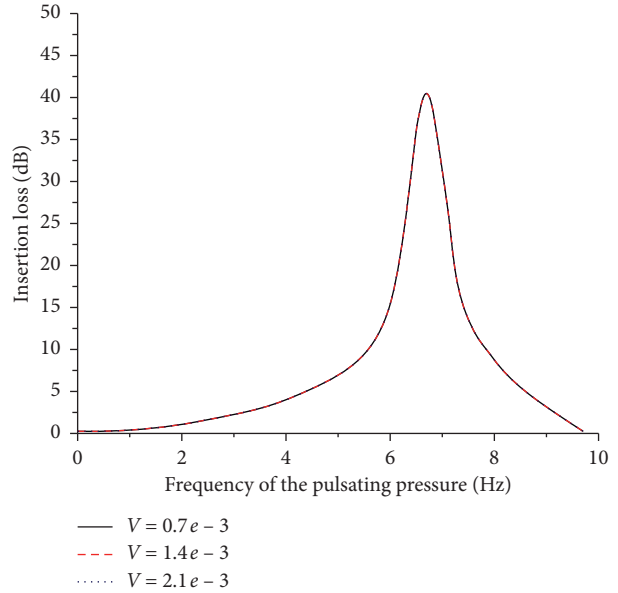

Figure 7: Effect of volume of the main cavity on insertion loss.

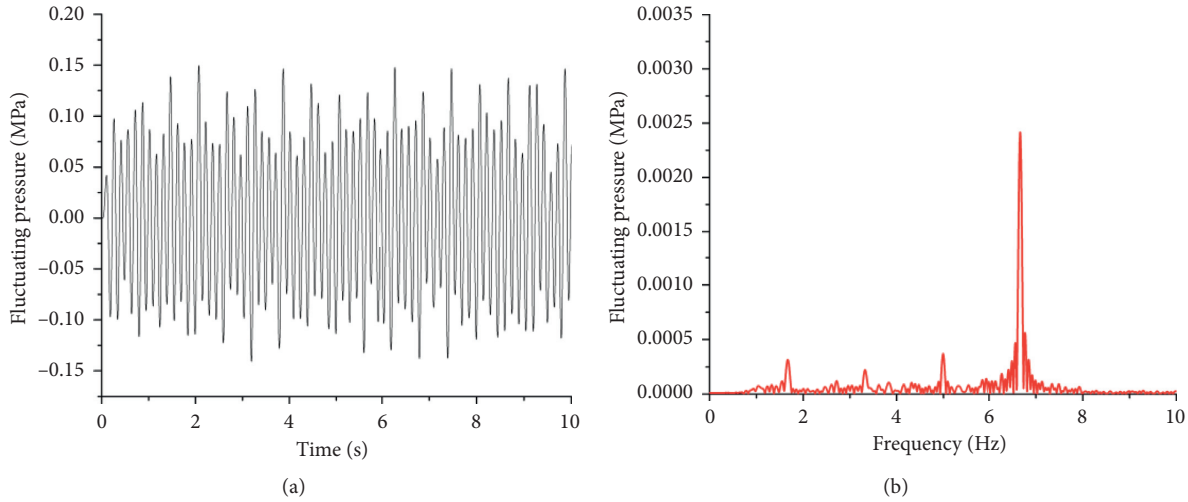

Figure 8: Time domain signal and frequency domain signal of fluctuating pressure under rated conditions. (a) Time domain signal. (b) Frequency domain signal.

It can be seen from Figure 8(b) that the frequency domain distribution of the fluctuating pressure of the linear-driving pump under the rated condition is relatively discrete; the fundamental frequency of the fluctuating pressure is 1.67 Hz, which is the same as the operating frequency of a single linear-driving pump. The amplitude of the fluctuating pressure at the fourth harmonic frequency is the largest. In order to maximize the attenuation of the fluctuating pressure, the fourth harmonic frequency, 6.67 Hz, was selected as the design frequency of the attenuator.

Combined with the analysis of the fluctuating pressure frequency under the rated working condition of the linear-driving pump and the frequency characteristics of the circular elastic sheet, the thickness of the sheet was selected to be 0.03 mm and the radius was 36 mm. Under this condition, the normal fundamental frequency of the sheet was 6.67 Hz. Since the volume of the main cavity has little effect on the performance of the attenuator, the attenuator size should be minimized under the premise of ensuring the cooperation between the components. The length and width of the casing were 122 mm, and the volume of the main cavity was 0.7 L. The prototype of pressure-fluctuating attenuator is illustrated in Figure 9.

Figure 9: Prototype of pressure-fluctuating attenuator.

4. Experimental Study

4.1. Performance Test Method. After the pressure-fluctuating attenuator was inserted into the pipeline system of linear-driving pump, the system will be loaded by the throttle valve. The fluctuating pressure of the fluid in the pipe acts on the circular elastic sheet to cause vibration of the sheets. Under the interaction of the sheets and the fluid, the fluctuating pressure will be consumed, and the pressure pulsation amplitude in the pipeline will be reduced. A pressure transmitter was installed on the pipeline behind the pressure-fluctuating attenuator to shield the external electromagnetic signal interference, the signal isolator was connected in series in the output loop, and the oscilloscope was connected to the isolator output loop to collect the signal. The performance test system for the pressure-fluctuating attenuator is shown in Figure 10, which mainly includes PMAC controller, linear-driving pump, relief valve, pressure fluctuating attenuator prototype, throttle valve, pressure transmitter, and turbine flow meter.

As the core component of the fluctuating pressure signal acquisition, the pressure transmitter was powered by a 24 V DC stable power supply. Under the external pressure (0–15 MPa), the transmitter will output a proportional current signal (4–20 mA). To avoid common mode interference from the external magnetic field and electric field, the signal isolator will be connected in series to the output circuit of the transmitter. The isolator uses current as the input signal and will output the voltage signal (0–10 V) according to the magnitude of the current. The ratio conversion from the pressure signal to the current signal and then from the current signal to the voltage signal was realized. The signal can be acquired by connecting the oscilloscope to the output loop of the isolator.

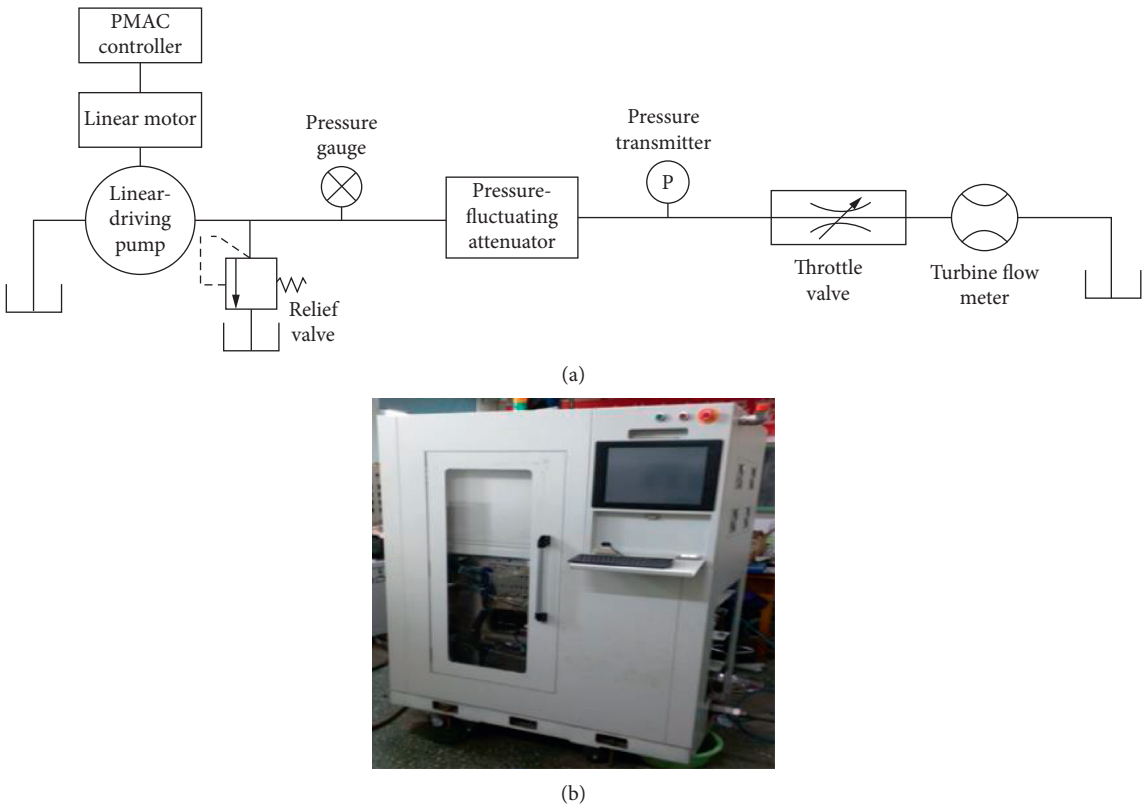

Figure 10: Diagram of performance test of the pressure-fluctuating attenuator. (a) Performance test system. (b) Linear-driving pump.

4.2. Performance Test Results and Analysis. To study the attenuation performance of the attenuator on the fluctuating pressure of the linear-driving pump and the correctness of the mathematical model of the attenuator, the specific test steps were arranged as follows:

(1) The motor was controlled by the upper computer software to operate according to the rated frequency. The throttle valve was adjusted to make the system load 1–5 MPa, respectively. The output voltage signal of the signal isolator was collected when the system runs smoothly under load conditions.

(2) Replace the attenuator with a stainless-steel tube of the same length as the attenuator into the piping system of the linear-driving pump, and adjust the throttle valve and repeat step (1) to collect the pulsating pressure signals of the same measuring point under different load conditions.

(3) The FFT of the signal data was used to obtain the frequency domain distribution of the pulsating pressure of the measuring point under different load conditions when the stainless-steel tube and the attenuator were installed, respectively.

When the linear-driving pump was under the rated working condition (that is, the operating frequency was 1.67 Hz and the load was 5 MPa), the frequency domain distribution of the pulsating pressure of the measuring point is shown in Figure 11. To further study the performance of the pressure-fluctuating attenuator, the signal data collected under different load conditions are analyzed and compared, and the frequency domain distribution is obtained, as shown in Figure 12.

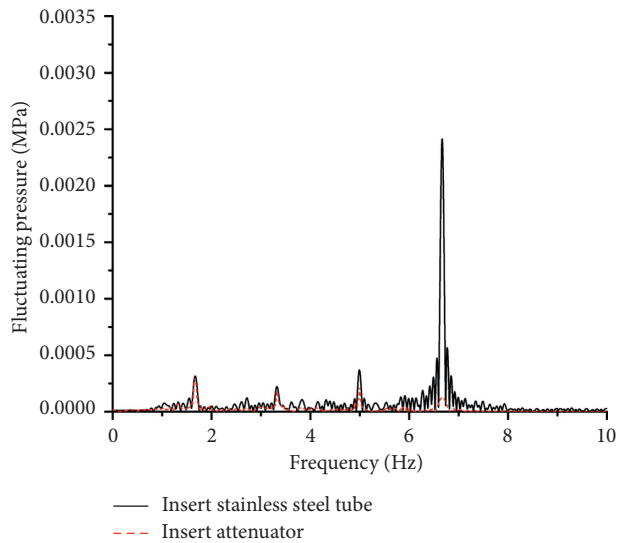

Figure 11: Signal of fluctuating pressure in frequency domain under rated condition.

As shown in Figures 11 and 12, when the linear-driving pump keeps the operating period constant, the fundamental frequency of the fluctuating pressure is correspondingly

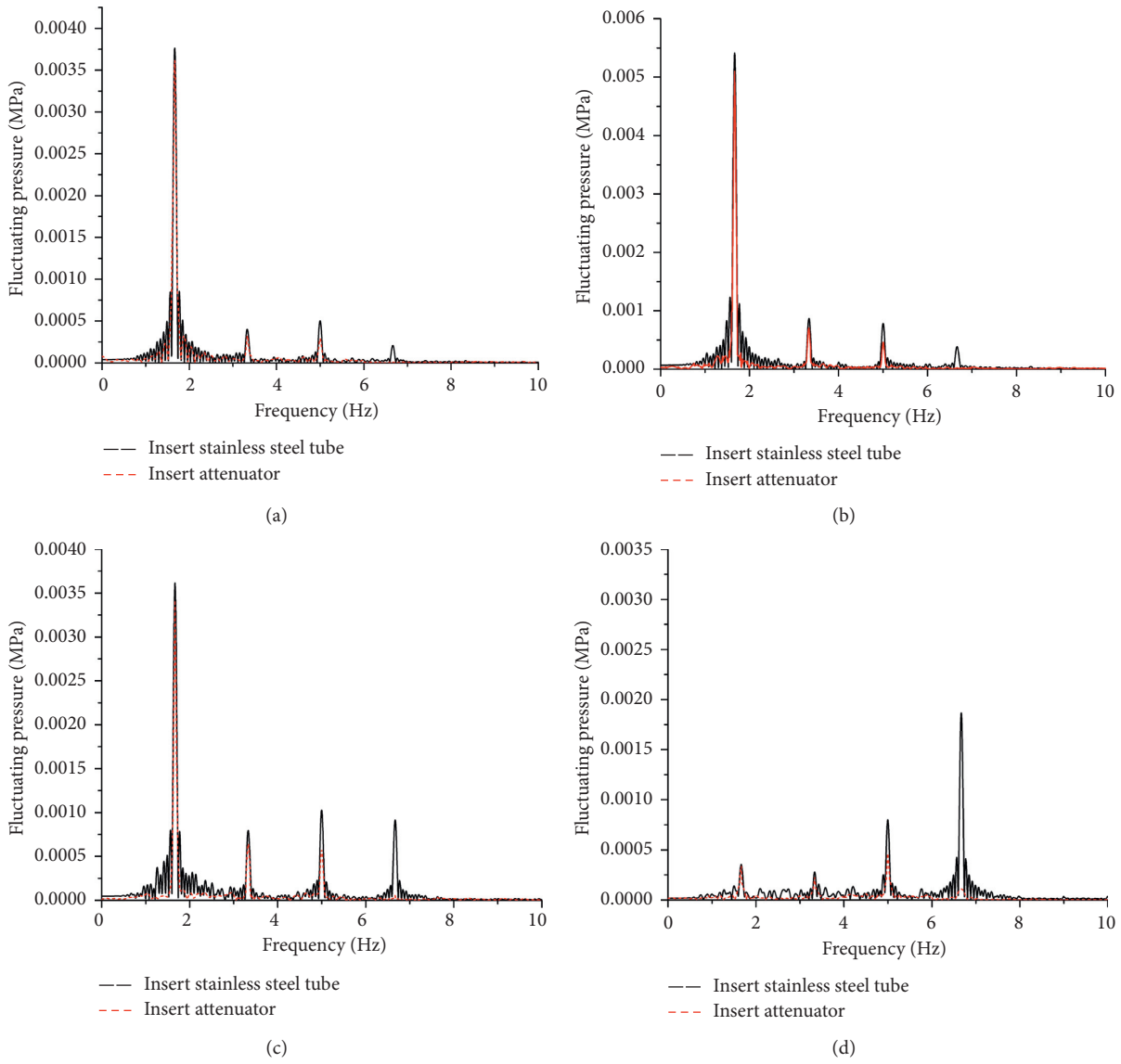

Figure 12: Frequency domain characteristics of fluctuating pressure with different loads. (a) Load = 1 MPa. (b) Load = 2 MPa. (c) Load = 3 MPa. (d) Load = 4 MPa.

unchanged and equal to the operating frequency of the linear-driving pump. Under different load conditions, the amplitude of the fluctuating pressure fundamental frequency and each harmonic frequency are different. As the system load increases, the amplitude of the fluctuating pressure corresponding to the higher harmonic frequency gradually increases. When the load is 5 MPa, the amplitude of the fluctuating pressure at the fourth harmonic frequency is the largest; meanwhile, the attenuation amplitude of the fluctuating pressure is the largest at the fourth harmonic frequency.

5. Results and Discussion

The insertion loss corresponding to each frequency at different loads are shown in Table 3. The natural frequency of the circular elastic sheet in the pressure-fluctuating attenuator was designed to be 6.67 Hz; the insertion loss of the pressure fluctuating attenuator was maximized at 6.67 Hz under different load pressure conditions. The expected vibration attenuation effect was achieved. As the load pressure increases, the insertion loss of the pressure-fluctuating attenuator remains substantially unchanged.

Table 3: Insertion loss (dB) corresponding to each frequency with different loads.

The frequency of pulsating pressure (Hz)	Load pressure (MPa)				
	1	2	3	4	5
1.67	0.43	0.41	0.44	0.43	0.4
3.33	1.65	1.53	1.61	1.48	1.57
5	4.42	4.61	4.53	4.38	4.68
6.67	25.3	24.7	25.6	26.4	26.1

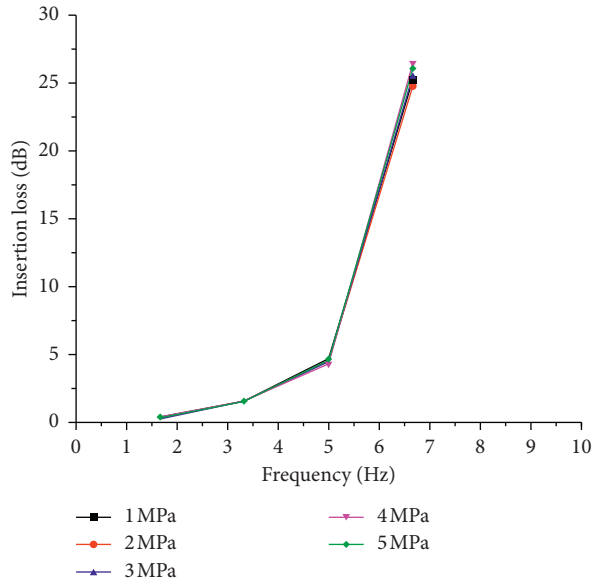

Figure 13: Performance curve of the attenuator with different loads.

The fluctuating pressure fundamental frequency and the insertion loss value corresponding to each harmonic frequency under each load condition were fitted to obtain an attenuator performance curve, as shown in Figure 13.

As shown in Figure 13, when the linear-driving pump operated under rated conditions, the insertion loss corresponding to the fundamental frequency and harmonic frequency of the fluctuating pressure becomes larger as the number of harmonics increases, and the maximum insertion loss at the fourth harmonic frequency is 26.1 dB. With the increase of harmonic frequency, the insertion loss trend of the pressure-fluctuating attenuator is basically identical under different load pressures. The variation trend of the insertion loss of each frequency point is the same as the simulation result, the expected effect is achieved. The correctness of the theoretical model of the attenuator is verified.

At the same time, with the change of system load, the insertion loss corresponding to the fundamental frequency of the fluctuating pressure and the harmonic frequency points remains basically unchanged. This is because when the running speed of the linear-driving pump is constant, the fundamental frequency and the harmonic frequency of the pulsating pressure interacting with the circular elastic sheet are also determined. The change in load pressure will have the same tendency to affect the amplitude of the fluctuating pressure at each frequency point when the stainless-steel tube and the attenuator are inserted. Therefore, there will be no significant change in the insertion loss associated with the ratio of the fluctuating pressure amplitude. In addition, in order to control the fluctuating pressure amplitude at 1.67 Hz under the load conditions of 1 MPa and 2 MPa, the circular elastic sheets with higher insertion loss at frequency of 1.67 Hz should be designed. By connecting circular elastic sheets with low-frequency suppression capability and high-frequency suppression capability in series to the pressure-fluctuating attenuator, the flow-induced vibration of the linear-driving pump at the fundamental frequency and the fourth harmonic frequency will be better suppressed, ensuring that the pipeline has a lower vibration amplitude under different load conditions.

6. Conclusions

This paper studies the vibration reduction measures of the pipeline system of the linear-driving pump. A new type of pressure-fluctuating attenuator with a circular elastic sheet was proposed. The natural frequency characteristics of the circular elastic sheet were analyzed, and the mathematical model of the pressure-fluctuating attenuator was established. The effect of relevant parameters on attenuation performance was investigated through simulation. The prototype was developed and the attenuation performance test was carried out. The experiment proves that the prototype has the best attenuation effect on the amplitude at the fourth harmonic frequency of the fluctuating pressure under rated conditions. The conclusions are as follows:

(1) According to the working principle of the attenuator, the radius of the circular elastic sheet has a great influence on the performance of the pressure-fluctuating attenuator. As the radius increases, the frequency of the fluctuating pressure corresponding to the peak of the attenuator insertion loss gradually decreases. The volume of the main cavity of the attenuator has little effect on the performance of the attenuator.

(2) When the linear-driving pump was operated under rated conditions, the pressure-fluctuating attenuator has the best suppression effect on the pulse pressure of 6.67 Hz, and the insertion loss was 26.1 dB. The experimental conclusions are in complete agreement with the simulation results. [27]

Data Availability

The datasets generated or analyzed to support the findings of this study are available from the corresponding author on reasonable request.

Conflicts of Interest

The authors declare that they have no conflicts of interest.

Authors' Contributions

Songlin Nie carried out conceptualization, project administration, writing review, and editing. Lianwei Li carried out the formal analysis and helped with software. Hui Ji performed data curation and helped with methodology and writing the original draft. Fanglong Yin carried out investigation and helped with software. Zhaoyi Dai carried out formal analysis, investigation, and writing review, and editing

Acknowledgments

This research was funded by the Beijing Natural Science Foundation (Grant no. 3182003), Equipment Pre-research Project of 2017 (Grant no. 61402100104), National Natural Science Foundation of China (Grant nos. 51905011, 51975010 and 51705008), Beijing Municipal Science and Technology Project (Grant nos. KM201810005014 and KM201910005033), International Research Cooperation Seed Fund of Beijing University of Technology (Grant no. 2018B17), and CSIC Key Laboratory of Thermal Power Technology Open Foundation (Grant no. TPL2017BB010) for their funding for this research. The authors would also like to thank Mr. Guo Yuewei and Dr. Huang Yeqin for their help in prototype design, simulation, and experiment.

References

[1] L Bai, L. Zhou, C. Han et al., "Numerical study of pressure fluctuation and unsteady flow in a centrifugal pump," *Processes*, vol. 7, no. 6, p. 354, 2019.

[2] L. Bai, L. Zhou, X. P. Jiang et al., "Vibration in a multistage centrifugal pump under varied conditions," *Shock and Vibration*, vol. 2018, Article ID 2057031, 9 pages, 2019.

[3] Z. Y. He, Q. H. He, and Z. G. Li, "Research on pressure pulsation suppression method of pump source hydraulic system research," *Lifting and Transport Machinery*, vol. 211, no. 10, pp. 24–26, 2010.

[4] C. H. Zhou, *Pump-motor Closed Hydraulic System Pressure Pulsation System Research*, Central South University, Changsha, China, 2012.

[5] G. Y. Chen, H. T. Zhou, and W. Zhou, "Expanded muffler reduces pipeline fluid noise experimental research," *Noise and Vibration Control*, vol. 5, no. 6, pp. 47–78, 2000.

[6] J. H. Fang, Y. Q. Zhou, X. D. Hu et al., "Fluid simulation of expanded muffler and aerodynamic performance study," *Journal of System Simulation*, vol. 21, no. 20, pp. 6399–6404, 2009.

[7] E. Kojima and T. Ichiyanagi, *Development Research of New Types of Multiple Volume Resonators. Bath Workshop on Power Transmission and Motion Control*, University of Bath, England, UK, 1998.

[8] Z. C. Luo, *Fluid Network Theory*, Mechanical Industry Publishing Society, Beijing, Germany, 1988.

[9] X. R. Zeng and J. C. Zhang, "Research on porous concentric hydraulic muffler," *Machine and Hydraulics*, vol. 18, no. 1, pp. 41–43, 1990.

[10] W. Bi, Z. S. Liu, H. J. Liu et al., "Study on acoustic characteristics of impedance compound muffler," *Automotive Engineering*, vol. 34, no. 7, pp. 633–637, 2012.

[11] W. Zhang, J. Yu, S. Li et al., "Simulation and experimental research on pressure pulsation attenuator research," *Hydraulics and Pneumatics*, no. 6, pp. 47–50, 2011.

[12] M. Josef, "A novel compact pulsation compensator to reduce pressure pulsations in hydraulic systems," in *Proceedings of Icanov-International Conference on Acoustics, Noise and Vibration*, Ottawa, Canada, January 2001.

[13] S. H. He, X. Z. Wang, Z. Y. He et al., "Thin plate vibrating hydraulic pulsation research on filter characteristics of reducer," *Mechanical Engineering*, vol. 49, no. 3, pp. 148–153, 2013.

[14] Q. Q. Sang, *Multi-thin Plate Vibrating Pulsation Attenuator Filtering Mechanism and Characteristic Analysis*, Changsha University of Science and Technology, Changsha, China, 2013.

[15] R. Sripriya, G. Karl, and M. John, "Theoretical study of structural acoustic silencers for hydraulic systems [J]," *Journal of the Acoustical Society of America*, vol. 111, no. 5, pp. 2097–2108, 2002.

[16] Z. P. Ren and S. P. Cao, "Dynamic analysis and simulation calculation of resonance muffler absorbing pressure pulsation," *Machine and Hydraulics*, vol. 34, no. 2, pp. 116-117, 2006.

[17] Y. Zhang, *Research on Characteristics of Pressure Pulsation Attenuator in Hydraulic System [D]*, Zhejiang University, Hangzhou, Zhejiang, China, 2010.

[18] S. H. He, Y. W. Xiong, and W. Wang, "Research on filtering characteristics of hydraulic pulsation attenuator based on biomimetic principle of cochlear basement membrane," *Journal of Mechanical Engineering*, vol. 52, no. 4, pp. 171–177, 2016.

[19] X. P. Dong, G. F. Bai, and K. Liu, "Study on sound absorption properties of elastic current-carrying sheet structure," *Journal of Acoustics*, vol. 32, no. 5, pp. 418–424, 2007.

[20] G. H. Du and Z. M. Zhu, *Acoustic Foundation*, Nanjing University Press, Nanjing, China, 2001.

[21] W. H. Peake and E. G. Thurston, "The lowest resonant frequency of a water-loaded circular plate," *The Journal of the Acoustical Society of America*, vol. 26, no. 2, pp. 166–168, 1954.

[22] B. Xiao, *Study on Fluid Pulsation Suppression of Rubber Pipeline System in Resin Anchoring Agent Production Line*, Taiyuan University of Technology, Taiyuan, China, 2015.

[23] Z. X. Wang, *Analysis of Filter Characteristics of Thin Plate Vibrating Fluid Filter*, Changsha University of Science and Technology, Changsha, China, 2012.

[24] Y. J. Hao, *Mechanical Analysis of the Interaction between Elastic Thin Plates and Fluids*, Yanshan University, Qin Huangdao, Hebei, China, 2010.

[25] C. G. Zhou, B. L. Liu, and X. D. Li, "Cavity wall elasticity to water Helmholtz influence of acoustic characteristics of vibrator: equivalent concentration parameter model of cylindrical cavity," *Journal of Acoustics*, vol. 32, no. 5, pp. 427–433, 2007.

[26] K. L. Xing, S. Liu, S. H. Ge et al., "Evaluation method of attenuation effect of pressure pulsation attenuator," *Mechanical Research and Application*, vol. 11, no. 4, pp. 6–9, 1998.